Research Square

Preprints are preliminary reports that have not undergone peer review.
They should not be considered conclusive, used to inform clinical practice,
or referenced by the media as validated information.

CAP1 is a gate keeper to maintain the homeostasis of human endothelial cells by formation of the triple complex with adenylyl cyclase and caveolin

Hyo-Soo Kim

hyosoo@snu.ac.kr

Seoul National University Hospital https://orcid.org/0000-0003-0847-5329

Sahmin Lee

University of Ulsan College of Medicine

Hyun-Chae Lee

Seoul National University Hospital

You Ji Kim

Seoul National University Hospital

Soobeom Lee

Seoul National University Hospital

Dasom Shin

Seoul National University Hospital

Joonoh Kim

Seoul National University Hospital

Jaewon Lee

Seoul National University Hospital https://orcid.org/0000-0002-9400-5384

EunByule Choi

Seoul National University Hospital

Hyun-Duk Jang

Seoul National University Hospital https://orcid.org/0000-0002-7126-3647

Han-Mo Yang

Seoul National University Hospital https://orcid.org/0000-0002-1548-2351

Yoo-Wook Kwon

Seoul National University Hospital https://orcid.org/0000-0003-2418-429X

Article

Keywords: Adenylyl cyclase-associated protein1, resistin, endothelial cell, inflammation, caveolin

Posted Date: April 28th, 2026

DOI: https://doi.org/10.21203/rs.3.rs-9333239/v1

License: This work is licensed under a Creative Commons Attribution 4.0 International License.
Read Full License

Additional Declarations: There is no conflict of interest

Abstract

Adenylyl cyclase-associated protein1 (CAP1) is a human resistin receptor that plays a key role in mediating monocyte actions and connecting chronic inflammation to cardio-metabolic diseases. However, its role in endothelial-monocyte interactions and adenylyl cyclase (AC) regulation remains unclear. We demonstrate that CAP1 forms a complex with adenylyl cyclase 3 (AC3) and caveoline-1 (CAV1) in lipid rafts membrane of endothelial cells (ECs), a triple complex of CAP1-AC3-CAV1 that maintains AC3 in a suppressed state. Knockdown of CAP1 in ECs disturbs the formation of AC3-inhibitory triple complex, leading to AC3 activation, cAMP-PKA-CREB signaling, and NF-κB-mediated upregulation of ICAM-1 and VCAM-1 on ECs facilitating monocyte adhesion, as well as disruption of mitochondria and barrier functions of ECs. Resistin treatment to ECs recapitulates CAP1 knockdown by disassembling the AC3-inhibitory triple complex of CAP1-AC3-CAV1, leading to AC3 activation. In the in vivo experiment using CAP1+/- mice with normal monocytes introduced from WT bone marrow transplantation, CAP1 knockdown in ECs significantly increased monocyte extravasation and infiltration toward chemoattractant Carrageenan, leading to aggravation of inflammation. These findings identify CAP1 on ECs as a gate keeper of their homeostasis regulating endothelial-leukocyte interactions as well as barrier functions via mitochondria, implying new mechanism how endothelial dysfunction induce inflammatory diseases.

INTRODUCTION

Metabolic diseases are strongly linked to chronic low-grade inflammation, and recent studies have established a direct cause-and-effect relationship between the two conditions[1]. Excess nutrients drive metabolic dysfunction, which in turn initiates inflammation, contributing to obesity, insulin resistance, and atherosclerosis[2]. Among potential mediators, human resistin has emerged as a key factor, as its elevated serum levels are consistently observed in patients with metabolic inflammation[3-6].

Resistin is a 12.5 kDa cysteine-rich adipokine that was originally reported to be secreted from adipocytes and to mediate insulin resistance in mice[7]. However, our previous work demonstrated that in humans, resistin is predominantly secreted by monocytes/macrophages rather than adipocytes and promotes atherosclerosis by upregulating adhesion molecules on endothelial cells (ECs), monocytes, and smooth muscle cells[8]. We further identified cyclase-associated protein 1 (CAP1) as a functional receptor for human resistin, which activates the cAMP-PKA pathway in monocytes[9]. Additionally, we found that resistin-CAP1 signaling induces mitochondrial fission and dysfunction, contributing to diabetes in the context of a high-calorie diet[10]. Intriguingly, we found the presence of circulating human monocytes that express the endocannabinoid receptor (CB1R) and secrete resistin upon stimulation of endocannabinoid (2-AG)[11]. These double-positive (CB1R and resistin expressing) monocytes are attracted to obese tissue having rich endocannabinoids, and then secrete resistin and activate CAP1, leading to inflammation or mitochondrial dysfunction of the cells in the obese fat, liver, or muscle leading to metabolic syndrome.

Thus, selective blocking of resistin-CAP1 binding may be a useful strategy to prevent the progression of atherosclerosis or diabetes.

Cyclase-associated protein (CAP) was first discovered in yeast cells and interacts with adenylyl cyclase as its name indicates[12]. Recently, we reported that CAP1 on hepatocytes also binds to PCSK9 whose Cysteine-Rich Domain has structural similarity to C terminal portion of resistin trimer, leading to internalization and degradation of LDL-receptor and increase of blood cholesterol level[13]. Furthermore, in monocyte and macrophages, the interaction of PCSK9 with CAP1 induces their activation and inflammation, leading to aggravation of atherosclerosis even in LDL-receptor knockout mouse[14]. These results suggest that CAP1 having multiple ligands such as resistin and PCSK9 plays an important role in inflammation and atherosclerosis where ECs play a major role. But CAP1 role in ECs remained unexplored.

Here, we found that CAP1 on ECs act as a critical regulator of inflammation. In normal conditions of ECs, CAP1 forms a suppressive triple complex with adenylyl cyclase (AC) and caveolin-1 (CAV1), which inhibits AC activity within caveolae of lipid raft membrane of ECs, maintaining basal low level of adhesion molecules. However, when CAP1 is knocked down in ECs, it disturbs the formation of AC-inhibitory triple complex (CAP1-AC3-CAV1) leading to activation of AC3 followed by PKA, NF-κB activation, and induction of adhesion molecules as well as disruption of mitochondria and barrier structure of ECs. Interestingly, resistin treatment to ECs recapitulates CAP1 knockdown by disassembling the AC-inhibitory triple complex (CAP1-AC3-CAV1) through binding to CAP1, leading to activation of AC. This mechanism is distinct from monocytes, where resistin directly activates AC via CAP1 to drive cytokine release. Moreover, *in vivo* experiment using $CAP1^{+/-}$ mice, CAP1 knockdown in ECs significantly increased monocyte extravasation and infiltration toward chemoattractant, leading to aggravation of inflammation. These findings identify CAP1 on ECs as a gate keeper of their homeostasis regulating endothelial-leukocyte interactions as well as barrier functions via mitochondria, providing critical insights into immune cell transmigration and inflammation in atherosclerosis and metabolic diseases, with potential implications for therapeutic intervention.

METHODS

Detailed methods are described in the Supplementary Information.

Animal Experiments

All animal experiments were approved (#SNU-140528-1-5) by the IACUC at Seoul National University Hospital. Age-matched (9–10 weeks) $CAP1^{+/-}$ mice were used, with wild-type mice as controls. As previously reported, homozygous deletion of Cap1 results in embryonic lethality, whereas $Cap1^{+/-}$ mice are viable and phenotypically normal[10,13-15]. Details on Carrageenan-induced Edema Formation and Bone Marrow Transplantation are in the supplemental information.

Cell Culture and Transfection

HUVECs (Lonza) were cultured in EGM-PLUS Medium (GIBCO) and used at passages 5–6. mFc-conjugated hResistin plasmid was transfected into HUVECs using polyethylenimine (PEI).

RNA Interference and Adenoviral Transduction

CAP1 knockdown was performed using siRNA (QIAGEN) with HiPerFect. Target sequence: 5'-AAACCGAGTCCTCAAAGAGTA-3'. siRNA (1 μg) was transfected per 2.5×10^5 cells. Human CAP1 was cloned into pAdTrack-CMV (GFP-tagged) and transferred into pAdEasy-1 for adenoviral transduction (MOI 100).

cAMP ELISA

HUVECs were starved in 1% FBS-EBM (2 h) before treatment with recombinant human resistin (100 ng/ml, 5 min–2 h), forskolin (50 mM, 30 min), or isoproterenol (10 min). Cyclic AMP levels were measured using Parameter™ cAMP ELISA (R&D).

Transmission Electron Microscopy (TEM)

HUVECs were fixed with 2% glutaraldehyde and 2% paraformaldehyde in 0.1 M phosphate buffer (pH 7.4) for 2 h at 4°C. After post-fixation with 1% osmium tetroxide for 1 h, samples were dehydrated in a graded ethanol series and embedded in Spurr's resin. Ultrathin sections (70 nm) were cut using an ultramicrotome (Leica), stained with uranyl acetate and lead citrate, and examined using a transmission electron microscope (JEOL, JEM-1400) at 80 kV.

Endothelial Permeability Assay

HUVECs were seeded onto Transwell inserts (0.4 μm pore size, Corning) and cultured until a confluent monolayer was formed. After treatment with CAP1 siRNA or resistin (100 ng/mL), FITC-dextran (4 kDa, 1 mg/mL, Sigma-Aldrich) was added to the upper chamber. After 30 min of incubation, the fluorescence intensity of the medium in the lower chamber was measured using a microplate reader (excitation 490 nm, emission 520 nm).

Measurement of Intracellular ROS and Mitochondrial ROS

Mitochondrial and cellular reactive oxygen species (ROS) levels were detected using CellROX™ Deep Red Reagent and MitoSOX™ Red Mitochondrial Superoxide Indicator (Thermo Fisher Scientific), respectively. Cells were treated with reagents as indicated, incubated with 5 μM CellROX or 5 μM MitoSOX for 30 min at 37°C in the dark, and washed with PBS. Fluorescence images were captured using a Leica STED CW inverted confocal microscope.

Carrageenan-induced Paw Edema Model

The in vivo inflammation assay was designed with three experimental conditions as outlined in Figure 6A. First, to determine the baseline edema response (Experiment I), 1% λ-carrageenan was injected into WT and CAP1+/− mice without adenoviral transduction or monocyte transfer. To trace monocyte infiltration (Experiment II) and assess the effect of hyper-resistinemia (Experiment III), we established a comprehensive model. For hyper-resistinemia, adenoviral human resistin (1×10^9 pfu per mouse) was systemically administered to mice via intracardiac injection on Day 0. Four weeks (28 days) post-transduction, normal monocytes isolated from WT mice were labeled with DiI and systemically transplanted into the recipient mice via intracardiac injection. Immediately following monocyte transfer, 50 µL of 1% λ-carrageenan (w/v in saline) was injected into the sub-plantar region of the hind paw to induce inflammation, while an equal volume of normal saline was injected into the contralateral paw as a control. The paws were harvested 18 hours after the carrageenan injection (Day 29). The depth of edema and the number of infiltrated DiI-labeled monocytes within the edematous tissues were quantified.

Bone Marrow Transplantation (BMT)

To investigate whether the downregulation of CAP1 specifically in endothelial cells promotes monocyte trans-endothelial migration in vivo, we generated bone marrow chimeric mice following the timeline outlined in Figure 7A. On Day 0, WT and CAP1+/− recipient mice were subjected to sub-lethal irradiation (7.5 Gy) using a Cesium-137 irradiator to ablate endogenous bone marrow. Donor bone marrow cells were harvested from GFP-transgenic mice (C57BL/6-Tg [CAG-EGFP]). A total of 5×10^7 GFP(+) bone marrow cells were systemically transplanted into the irradiated recipient mice via intracardiac injection.

On Day 20, successful engraftment was verified by analyzing the percentage of donor-derived GFP(+)/CD45(+) cells in the peripheral blood using flow cytometry (FACS). Upon confirmation of reconstitution, on Day 21, hyper-resistinemia was induced by systemic administration of adenoviral human resistin (1×10^9 pfu per mouse).

On Day 28 (one week after viral transduction), 50 µL of 1% λ-carrageenan was injected into the sub-plantar region of the hind paw to trigger local inflammation. Finally, on Day 29 (18 hours post-carrageenan injection), the paws were harvested, and edema depth, paw volume, and GFP(+) monocyte infiltration were quantified.

In Vivo Vascular Permeability Assay

To assess endothelial barrier function in vivo, we utilized a mustard oil-induced vascular leakage model. Evans Blue dye was dissolved in Dulbecco's Phosphate-Buffered Saline (DPBS) to a final concentration of 2%. Mice were anesthetized, and 200 µL of the Evans Blue solution was administered via intra-cardiac injection. One minute after the dye injection, vascular leakage was chemically induced by the topical application of mustard oil (diluted to 5% in mineral oil). The solution was applied to both the dorsal and ventral surfaces of the ear using a cotton swab. To ensure a sustained inflammatory response, mustard oil was reapplied 15 minutes later. Mice were euthanized 30 minutes after the initial mustard oil application, and the ear tissues were harvested. To quantify the extravasated dye, the tissues were

immersed in 600 µL of formamide and incubated overnight at 55°C to extract the Evans Blue. The concentration of the extracted dye was determined by measuring absorbance spectrophotometrically at 610 nm.

Statistical Analysis

All experiments were performed at least three times. Data are presented as mean ± SEM. Student's t-test was used, and $p < 0.05$ was considered statistically significant.

RESULTS

CAP1, a functional receptor of human resistin, is necessary to control the expression of adhesion molecule in human ECs

To confirm CAP1 as a functional receptor of human resistin in ECs, two conditions needed to be met: direct binding between CAP1 and resistin, and CAP1's functional role in resistin-mediated signaling.

Immunoprecipitation assays using His-tagged CAP1 and c-Myc resistin-transfected cells demonstrated direct binding (Figure 1A). Additionally, in mouse Fc-tagged human resistin-transfected cells, native CAP1 co-localized with ectopically expressed resistin (Figure 1B). However, these experiments to confirm physical interactions were done using extrinsic vector expression, which may not fully reflect receptor-ligand dynamics in native cellular environments. To address this, we assessed resistin's ability to bind native membrane-localized CAP1 by using a neutralizing assay with recombinant CAP1. Resistin up-regulates the expression of ICAM-1 and VCAM-1 on ECs within its physiological serum concentration of 10 to 100 ng/mL[16,17]. Resistin treatment (50 ng/mL) significantly upregulated VCAM-1 expression, but pre-incubation with recombinant CAP1 at a fivefold molar excess reversed this effect (Figure 1C, D). These findings suggest that resistin interacts with membranous CAP1 and acts as an inflammatory cytokine by inducing adhesion molecules in ECs.

CAP1 knockdown induces adhesion molecule in human ECs

To further validate CAP1's functional role, we knocked down CAP1 using siRNA in HUVECs. Resistin treatment induced ICAM-1 and VCAM-1 expression, yet, unexpectedly, CAP1 knockdown did not block this effect (Figure 1E, F). "Exogenous application of CAP1 protein" to HUVEC competitively blocked resistin-induced adhesion molecule expression, while "endogenous CAP1 depletion" inside HUVEC by siRNA did not block but induce the adhesion molecules. Surprisingly, CAP1 knockdown alone increased ICAM-1 and VCAM-1 expression at both mRNA and protein levels, even in the absence of resistin stimulation (Figure 1G, H). To obtain a comprehensive view of the global transcriptional changes induced by CAP1 deficiency, we performed RNA sequencing (RNA-seq) on CAP1-knockdown HUVECs. The volcano plot highlighted a profound shift in the transcriptomic landscape (Figure 1I). Gene ontology and heatmap analyses revealed a broad upregulation of leukocyte adhesion molecules, including *SELP* (P-selectin), *SELL* (L-selectin), *SELPLG*,and *ICAM2* (Figure 1J), which was further validated by quantitative

real-time PCR analysis (Figure 1K). These results contrast with our previous findings in monocytes where CAP1 depletion reduced inflammatory responses of monocytes[9]. This suggests that CAP1's role as a receptor for human resistin may vary by cell type.

CAP1 binds to and suppresses adenylyl cyclase(AC) in the caveolin1(CAV1)-enriched lipid raft membrane in human ECs : CAP1-AC-CAV1 triple complex suppresses AC activation and maintains the homeostasis of ECs

To investigate and compare the distinct effects of CAP1 depletion between human ECs and monocytes, we examined its downstream targets, focusing on adenylyl cyclases (ACs) and cAMP synthesis[9]. The 10 AC isoforms exhibit tissue-specific expression patterns and unique mechanisms of action[18]. Thus, we hypothesized that CAP1 differentially regulates distinct AC isoforms depending on the cell type. Indeed, HUVECs and THP1 (monocyte cell line) showed different expression profiles of adenylyl cyclase isoforms. At the mRNA level, HUVECs showed high expression levels of AC3, AC4, AC6, and AC9, while THP1 predominantly expressed AC3, AC7, and AC9 (Figure 2A, B). Protein analysis further confirmed these differences: HUVECs expressed AC3 and AC5/6, while THP-1 cells expressed AC4 and AC7. Given the consistency between mRNA and protein data, we identified AC3 and AC6 as the dominant isoforms in HUVECs and AC7 as the major isoform in THP-1 cells (Figure 2C, D).

Notably, as AC5 and AC6 share nearly identical structures, they could not be distinguished via immunoblotting. However, since only AC6 was detected at the mRNA level in HUVECs, we attributed the AC5/6 protein signal to AC6 in this cell type. Collectively, these findings indicate that AC3 and AC6 are the predominant adenylyl cyclases in HUVECs, whereas AC7 is the principal isoform in THP-1 monocytes (Figure 2A–D).

Next, we examined the cellular distribution of AC isoforms and their localization within caveolae. Previous studies have reported that AC1, AC3, AC5/6, and AC8 localize to lipid rafts, whereas AC2, AC4, and AC7 are found in non-lipid raft regions[18]. Lipid raft localization plays a crucial role in caveolae-mediated regulation of signaling components, such as adenylyl cyclases, through caveolin (CAV) protein scaffolding. Our analysis revealed that CAV1 was significantly more abundant in HUVECs than in THP-1 cells. To further investigate AC localization, we fractionated lipid rafts (lane 2) from non-lipid raft regions (lane 3). This analysis identified AC3 and AC6 as being predominantly localized in the lipid raft layer of HUVECs, while AC7 was restricted to the non-lipid raft layer in THP-1 cells (Figure 2C, D). Notably, CAP1 was also found to co-localize with CAV1 in the lipid raft layer. These findings provide the first evidence of CAP1, AC3, AC6, and CAV1 co-localizing in endothelial cell lipid rafts.

To further assess CAP1's interaction with AC3 or CAV1 in lipid rafts, we performed immunoprecipitation of membrane proteins from HUVECs using an anti-CAP1 antibody (Figure 2E) and an anti-CAV1 antibody (Figure 2F). Both AC3 and CAV1 co-precipitated with CAP1, suggesting a functional association. Collectively, our data indicate that the well-developed caveolae in ECs facilitate CAP1 and AC3 localization within lipid rafts via direct interaction with CAV1—an interaction that is absent in monocytes.

Lastly, we investigated whether depletion of CAP1 or pharmacological disruption of caveolae could induce adhesion molecules in ECs. To assess the interaction between AC3 and CAV1 following CAP1 knockdown, we performed a Proximity Ligation in situ Assay (PLA). The interaction between AC3 and CAV1 was visualized as red dots, while CAP1 was indicated by green signals. As shown in Figure 2G, CAP1 knockdown reduced the interaction between AC3 and CAV1. Furthermore, knockdown of either CAP1 or CAV1 led to complex disassembly and AC3 de-inhibition, which in turn elevated ICAM-1 and VCAM-1 expression (Figure 2H). Similarly, pharmacological caveolae disruption using methyl-beta-cyclodextrin (MβCD) markedly increased ICAM-1 expression after 6 hours, coinciding with the phosphorylation of vasodilator-stimulated phosphoprotein (VASP), a key PKA substrate, as well as adhesion molecules (Figure 2I). All these findings suggest that CAP1 binds to AC and CAV1, leading to formation of triple complex CAP1-AC-CAV1 that is a gate keeper to inhibit AC, to suppress the expression of adhesion molecules on human ECs, and to maintain the normal function of ECs.

Signaling pathway for induction of adhesion molecules after CAP1 depletion is the cAMP-PKA-CREB and NF-κB activation in human ECs

Notably, We tested the hypothesis that CAP1 depletion disturbs the AC-inhibitory complex of CAP1-AC-CAV1, induces release of AC3 suppression, and cAMP elevation by conducting ELISA experiments. CAP1 knockdown alone was sufficient to significantly increase basal cAMP levels and markedly potentiated AC activity in response to forskolin, a direct AC activator, as well as isoproterenol, a β-adrenergic receptor agonist (Figure 3A, B). This implies CAP1's crucial role to maintain the inhibitory function of the CAP1-AC3-CAV1 complex on AC3 and cAMP synthesis. To further investigate the signaling pathways underlying ICAM-1 and VCAM-1 upregulation, we examined PKA activation, a primary downstream effector of cAMP, by assessing the phosphorylation of its key targets, VASP and CREB. Western blot analysis revealed that CAP1 knockdown significantly upregulated the expression of adhesion molecule (ICAM-1), concomitant with increased the phosphorylation of VASP (Ser157), indicating robust PKA activation (Figure 3C). Concurrently, we observed nuclear translocation of NF-κB subunits (p50, p-p65) and increased phosphorylation of CREB (Ser133) (Figure 3D), suggesting that the cAMP-PKA axis mobilizes these key transcription factors to induce inflammatory gene expression.

CAP1 depletion destabilizes endothelial barrier and facilitates monocyte extravasation

We investigated whether the upregulation of ICAM-1 and VCAM-1 induced by CAP1 depletion in ECs promotes leukocyte trans-endothelial migration. HUVECs, treated with CAP1 siRNAs for 24 hours, were cultured on Transwell inserts, and THP-1 cells were placed in the upper chamber (Figure 4A). Monocyte transmigration was significantly enhanced across ECs monolayer when CAP1 is knocked down in ECs (Figure 4B, C).

Since leukocyte extravasation requires not only adhesion but also the opening of the endothelial barrier, we next assessed endothelial permeability using a FITC-dextran assay. Notably, both CAP1 knockdown significantly increased para-cellular permeability (Figure 4D). Consistent with this, immunofluorescence staining revealed that the tight junction (ZO-1) proteins and the inter-endothelial junctional protein

(PECAM-1) were disrupted and fragmented under these conditions (Figure 4E), indicating destabilization of endothelial junctions. This structural destabilization was accompanied by a significant reduction in the protein level of PECAM-1, a key component for maintaining barrier integrity and mechano-transduction (Supplemental Figure 1).

To determine whether this barrier destabilization reflects a broader transcriptional reprogramming rather than a transient structural disturbance, we further interrogated our transcriptomic data on CAP1-knockdown HUVECs. Transcriptomic analysis revealed a significant downregulation of multiple gap junction proteins, including GJA4 (connexin 37), GJA5 (connexin 40), and GJA1 (connexin 43), which was further validated by quantitative real-time PCR analysis (Figure 4F-H). Given the essential role of connexins in maintaining endothelial cell–cell communication, junctional coordination, and barrier integrity, their coordinated suppression suggests that CAP1 is the pivotal molecule to maintain the barrier functions of ECs.

CAP1 depletion induces mitochondrial fission and oxidative stress leading to barrier dysfunction

We next explored the intracellular mechanism linking CAP1-AC3-CAV1 complex to barrier function, focusing on mitochondrial dynamics. Based on our previous finding that resistin-CAP1 axis induces PKA signaling and mitochondrial fission[10], we hypothesized that PKA activation by CAP1 depletion in ECs may induce mitochondrial fragmentation–associated oxidative stress, contributing to junctional instability.

Indeed, CAP1 knockdown markedly increased cellular ROS levels (Figure 5A). Consistent with this stress response, RNA-seq analysis also revealed that CAP1 knockdown upregulated interferon-stimulated genes, including RSAD2 and CMPK2 (Supplemental Figure 2A, B), which are known to exacerbate mitochondrial oxidative stress and metabolic dysfunction. Interestingly, this stress response was accompanied by a robust upregulation of the mitophagy receptor OPTN and lysosomal enzymes (CTSK, GBA, ACP5) (Supplemental Figure 2C-E) Concordantly, CAP1 depletion promoted recruitment of phosphorylated Drp1 (Ser616) to mitochondria (Figure 5B, C), a key driver of mitochondrial fission, as confirmed by 3D image quantification (Figure 5D, E). Ultrastructural analysis by transmission electron microscopy further confirmed severe mitochondrial damage, characterized by swelling and loss of cristae architecture (Figure 5F). Accordingly, mitochondrial ROS levels were significantly increased (Figure 5G).

Mechanistically, oxidative stress is known to destabilize adherens junctions, and we found that both CAP1 knockdown robustly induced phosphorylation of VE-cadherin, a hallmark of junctional disassembly (Figure 5H).

To validate the physiological relevance of these findings *in vivo*, we assessed vascular leakage using a mustard oil–induced permeability assay. $CAP1^{+/-}$ mice exhibited significantly increased Evans Blue extravasation compared with WT controls, indicating compromised vascular barrier integrity (Figure 5I, J).

CAP1 depletion is recapitulated by resistin treatment that 'disassembles' CAP1-AC3-CAV1 complex and activates AC

We hypothesized that the CAP1-AC3-CAV1 complex suppresses AC3 under basal state and that resistin activates AC3 by disrupting this complex. To test this, we performed Opti-prep density gradient centrifugation following resistin exposure. Notably, CAP1 levels in the lipid-raft fraction decreased within 30 minutes of resistin treatment and were nearly undetectable after 2 hours. Concurrently, Gαs accumulation in lipid rafts indicated AC activation and cAMP synthesis (Figure 6A).

Immunoprecipitation assays provided mechanistic insight into this "switch-off/switch-on" process. Under basal conditions, AC3 formed a stable complex with CAP1. Resistin treatment not only dissociated CAP1 from AC3 but, crucially, promoted the interaction between AC3 and Gαs (Figure 6B). Co-immunoprecipitation with anti-AC3 and anti-CAP1 antibodies demonstrated the separation of CAP1 and AC3, as well as CAV1 from CAP1. Immunofluorescent staining confirmed CAP1's co-localization with CAV1 at baseline, which was disrupted after resistin binding to CAP1 (Figure 6C, D). Collectively, these findings suggest that upon resistin binding, CAP1 is displaced from caveolae to the non-lipid raft or cytosolic fraction, leading to the disassembly of the CAP1-AC3-CAV1 complex and subsequent AC3 activation.

In cAMP ELISA experiments, Resistin treatment to HUVECs significantly and rapidly increased the intracellular cAMP levels within 10 minutes, followed by a sustained elevation up to 2 hours (Figure 6E). And then resistin treatment significantly upregulated the adhesion molecule (ICAM-1), concomitantly with phosphorylation of VASP (Ser157), indicating robust PKA activation (Figure 6F). Concurrently, we observed nuclear translocation of NF-κB subunits (p50, p-p65) and increased phosphorylation of CREB (Ser133) (Figure 6G), suggesting that the cAMP-PKA axis mobilizes these key transcription factors to induce inflammatory gene expression.

In trans-well migration experiment, resistin treatment enhanced monocyte transmigration across the endothelial monolayer (Figure 6I, J), increased para-cellular permeability (Figure 6K), disrupted the structural integrity of tight junction (ZO-1) accompanied by a specific decrease in PECAM-1 levels (Figure 6L, Supplemental Figure 1A). Regarding mitochondrial function, resistin treatment markedly increased cellular ROS levels (Supplemental Figure 3A), through mitochondrial fission by promoting phosphorylated Drp1 (Ser616) (Supplemental Figure 3B-E), a key driver of mitochondrial fission, as well as mitochondrial destruction reflected by swelling and loss of cristae architecture in EM (Supplemental Figure 3F). Such mitochondrial destruction and oxidative stress destabilizes adherens junctions, which was reflected by the result that resistin treatment induced phosphorylation of VE-cadherin (Supplemental Figure 3H).

All these findings well demonstrated that ECs' homeostasis is maintained by AC-inhibitory triple complex (CAP1-AC3-CAV1) formation in the lipid-raft membrane, which can be disturbed by CAP1 depletion or disassembled by resistin treatment.

CAP1 deficiency in ECs facilitates '*in vivo*' monocyte extravasation and aggravates local inflammation

We aimed to determine whether genetic CAP1 downregulation in ECs enhances *in vivo* monocyte trans-endothelial migration, as observed in our *in vitro* experiments. To this end, we used the carrageenan-induced edema formation model and examined the degree of inflammation in WT mice and $CAP1^{+/-}$ mice, the latter of which have reduced level of CAP1 (Figure 7A, Experiment I [Baseline]). To trace the extravasation of the circulating monocyte into the local inflamed tissue, DiI-labeled monocytes were prepared and systemically administered via intra-cardiac injection into WT or $CAP1^{+/-}$ mice. And then we injected 50 μl λ-carrageenan (1%, w/v) into sub-plantar space of hind paw (Figure 7A, Experiment II). In addition hyper-resistinemia was induced by adenoviral overexpression of human resistin four weeks prior to DiI-labeled WT monocytes injection (Figure 7A, Experiment III).

We measured the depth of edema and the degree of trans-endothelial monocyte infiltration in the hind paw where carrageenan was injected. To our surprise, paw edema after Carrageenan injection was significantly milder in $CAP1^{+/-}$ mice compared to WT controls (Figure 7B, C), which was accompanied by the greater infiltration of DiI-labeled monocyte into inflamed paw tissue (Figure 7D, E), consistent with our *in vitro* findings that CAP1 depletion in ECs upregulates adhesion molecules and promotes leukocyte migration. The paradox between less edema and more mono-macrophage infiltration in $CAP1^{+/-}$ mice was reproduced under hyper-resistinemic conditions (Figure 7F, G), suggesting impaired inflammatory function of CAP1-deficient monocytes in $CAP1^{+/-}$ mice. Thus, monocytes from the bone marrow of $CAP1^{+/-}$ mice were tested against monocytes from WT mice. Compared to WT monocytes, $CAP1^{+/-}$ monocytes exhibited reduced inflammatory gene expression and cytokine secretion, as confirmed by qRT-PCR and ELISA (Figure 7H, I). In collagen gel-based invasion assays, $CAP1^{+/-}$ monocytes compared with WT monocytes showed significantly diminished migration toward rhResistin or LPS (Figure 7J-L), confirming their attenuated activation capability.

Due to the unavailability of endothelial cell-specific CAP1 knockout mice, we established *in vivo* conditions where CAP1 is knocked down in ECs with supplementation of normal monocytes from WT mice in order to exclude the confounding influence of CAP1 deficient monocytes from CAP1 hetero-knockout mice. To directly assess the role of endothelial CAP1 in monocyte extravasation independent of monocyte function, we generated bone marrow chimeric mice by transplanting GFP-positive WT bone marrow cells into lethally irradiated WT or $CAP1^{+/-}$ recipients (Figure 8A, B). This model ensured that circulating monocytes were functionally normal while CAP1 was selectively deficient in ECs. In this setting, $CAP1^{+/-}$ mice exhibited greater infiltration of GFP-positive monocytes into inflamed tissue (Figure 8C-F) as well as more severe paw edema compared to WT controls (Figure 8G-H). Local inflammations and edema were aggravated by additional hyper-resistinemia after systemic injection of Adv-hResistin in this animal model (Figure 8I-J), which is well supported by the in-vitro results (Supplemental Figure 4).

Collectively, these findings support a comprehensive model (Figure 8K–M) in which CAP1 knockdown or resistin treatment disturbs the formation of AC-inhibitory triple complex (CAP1–CAV1–AC3), leading to

AC activation and cAMP accumulation. This signaling cascade exerts dual effects: (1) PKA-dependent upregulation of adhesion molecules (ICAM-1 and VCAM-1) (Figure 8K), and (2) PKA-mediated phosphorylation of Drp1, resulting in mitochondrial fission and ROS overproduction. The ensuing oxidative stress, together with transcriptional suppression of connexin-mediated gap junctions, destabilizes endothelial junctions and barrier integrity (Figure 8L), thereby facilitating monocyte extravasation and aggravating vascular inflammation (Figure 8M). Such phenotypes of CAP1 depletion are well recapitulated by resistin treatment that also 'disassembles' CAP1-AC3-CAV1 complex and activates AC, ultimately exacerbating endothelial barrier disruption and monocyte infiltration.

DISCUSSION

CAP1 is a key biphasic controller of adhesion molecules on human ECs

We previously demonstrated the direct binding between CAP1 and resistin in monocytes, which is an important mechanism how monocytes are activated and release cytokines leading to fat inflammation and metabolic syndrome[9]. In this study, we identified CAP1 as a receptor for human resistin in human ECs, crucially regulating adhesion molecules on ECs surfaces and governing the trans-endothelial migration of circulating monocytes towards inflamed tissues. CAP1 in ECs without stimulation of resistin acts as a barrier against monocyte extravasation and local inflammation because it forms the triple complex with AC and CAV1 leading to suppression of AC and inhibition of adhesion molecules. This mechanism is supported by the findings that CAP1 knockdown impairs formation of the AC-inhibitory triple complex (CAP1-AC-CAV1), leading to activation of AC, downstream signals, NFkB, and then induction of adhesion molecules on ECs. Thus CAP1 knockdown worsens monocyte trans-endothelial migration and extravasation into the inflamed tissues. Interesting point is that when resistin binds to CAP1, it dissembles the AC-inhibitory triple complex, leading to activation of AC and induction of adhesion molecules on ECs. Thus CAP1 is a biphasic controller of adhesion molecules' expression on ECs, trans-endothelial migration of monocytes, and vascular inflammation: 'turn-off inflammation' under normal basal condition, but 'turn-on inflammation' under resistin stimulation.

CAP1 binds to adenylyl cyclase-3 or -6 in the caveolin1-enriched lipid raft membrane in ECs: the formation of triple complex CAP1-AC-CAV1

We also identified critical differences in the regulatory mechanisms of CAP1 between ECs and monocytes. Previous studies showed that CAP1 is diffusely distributed in the cytoplasm, partly localized at the plasma membrane, and exceptionally in the mitochondria[9,19,20]. We found that CAP1 was localized in plasma membrane lipid rafts, and interacted with AC3 or AC5/6 in ECs, while it was localized in non-raft membrane and interacted with AC4 or AC7 in monocytes. Since lipid rafts are enriched with caveolae, we tested and confirmed the formation of triple complex, CAP1-AC3-CAV1 in the lipid raft membrane of ECs. Interestingly, activity of AC3 is suppressed in the triple complex of CAP1-AC3-CAV1 because of the steric hindrance against Gas protein access. But when ECs are treated with resistin,

resistin binds to CAP1, disassembles the triple complex, and expose AC3 to Gas protein, leading to activation of AC3 and downstream signals.

Regarding the association of AC and CAV1, some isoforms of the AC are known to be specifically localized at caveolae. However, there are conflicting reports whether caveolae inhibit or stimulate AC activity and downstream signal. The scaffold domain of caveolin was reported to directly inhibit AC3 and AC5 [21,22], and the disorganization of caveolae-associated β-adrenergic receptors and AC5/6 was reported to enhance AC activity and cAMP production[23]. These reports look well aligned with our findings that the activity of AC might be restrained in the caveolae but activated by disruption of complex. However, one paper argued that caveolin prompted AC6 to localize in the region close to beta-adrenergic receptors in caveolae and caused sensitization in a receptor-effector coupling manner[24]. Conflicting prior findings may stem from the differences in cell types, ligands, receptors, and AC isoforms. In our study, we screened ten AC isoforms and discovered that AC isoforms 1, 3, 5, 6, and 8 reside in caveolae. Notably, ECs primarily contain AC isoforms 3 and 6, which co-localize with CAP1 in caveolae, albeit in an inhibited state.

The impaired formation of triple complex of CAP1-AC3-CAV1 by CAP1 knockdown or its dis-assembly by resistin treatment leads to de-inhibition or activation of AC3 in ECs

Traditionally, cAMP signaling in ECs has been regarded as vasoprotective[25], contributing to barrier stabilization, cytoskeletal relaxation, and suppression of inflammatory activation through 'the tightly-regulated and spatially-confined cAMP signaling', particularly within caveolae microdomains and under transient stimulation conditions. However, according to the accumulating evidences, 'the sustained or spatially-dysregulated cAMP signaling' can exert paradoxical pro-inflammatory effects in ECs[26], especially when its compartmentalization is disrupted[27] or signaling duration is prolonged[28].

In this context, our findings indicate that the CAP1–CAV1–AC3 complex functions as a critical molecular brake that restrains both basal and agonist-induced adenylyl cyclase activity in ECs. The spatiotemporal control of cAMP signaling may be altered by the impaired formation of triple complex by CAP1 knockdown or the dis-assembling of triplex complex by resistin stimulation. Indeed, in cAMP ELISA experiments, resistin induces a rapid increase in intracellular cAMP within 10 minutes followed by sustained elevation for up to 2 hours, indicating not only acute activation but prolonged accumulation of cAMP. Notably, CAP1 knockdown alone was sufficient to significantly elevate basal cAMP levels and to potentiate adenylyl cyclase responsiveness to a direct AC activator forskolin as well as a β-adrenergic receptor agonist isoproterenol. These findings suggest that CAP1 contributes to the tonic suppression of AC3 activity, rather than serving solely as a passive scaffolding component.

Mechanistically, when AC3 is sequestered within the intact CAP1–AC3–CAV1 complex in caveolae, access of Gαs to AC3 appears to be hindered. Upon resistin binding, CAP1 trans-locates from caveolae lipid-rafts to non-lipid-raft membranes or the cytosol, leading to disassembly of the complex and relief of AC inhibition. This allows Gαs to efficiently bind and activate AC3, resulting in exaggerated and sustained

cAMP production and prolonged PKA activation, as reflected by persistent phosphorylation of VASP and CREB for over 24 hours.

Such sustained and de-compartmentalized cAMP/PKA signaling provides a mechanistic framework linking CAP1–AC3 complex disruption to endothelial dysfunction. While transient cAMP signaling is protective, prolonged activation has been reported to promote mitochondrial dysfunction, oxidative stress, and inflammatory endothelial activation[30]. Consistent with this model, we observed that CAP1 depletion or resistin treatment induced mitochondrial fission, ROS accumulation, and subsequent destabilization of endothelial junctions, including phosphorylation of VE-cadherin and reduction of PECAM-1. Together with transcriptional suppression of connexin-mediated gap junctions, these effects converge to compromise endothelial barrier integrity, thereby facilitating monocyte extravasation and amplifying vascular inflammation.

The precise molecular basis by which resistin-bound CAP1 fails to bind again to the dissociated AC3 or CAV1 remains unclear. Our previous work demonstrated that CAP1 contains distinct AC-binding domains for AC3/CAV1 and an SH3-binding domain for resistin, raising the possibility that resistin binding induces steric hindrance or conformational changes that prevent reassembly of the inhibitory complex. Further structural and biophysical studies will be required to elucidate this mechanism.

In the current study, the signaling pathway after AC3 activation in ECs was cAMP-PKA-CREB and NF-κB activation. The connection between the PKA pathway and NF-κB activation remains unresolved. A sequential activation process was suggested, where cytosolic phospholipase A2α (cPLA2α) promotes PGE2 production leading to PKA-CREB activation while concurrently facilitating NF-κB phosphorylation through an unidentified kinase[29]. Another study indicates that PKA may directly phosphorylate the Ser276 site of the p65 NF-κB subunit in the presence of A kinase interacting protein 1 (AKIP1)[30]. Additionally, hypothesis would be that NF-κB activation could be triggered by upstream signaling events such as Gβγ activation. Further research is needed to determine whether CAP1-driven cAMP signaling in ECs aligns with any of these pathways.

Vascular inflammation after disruption of CAP1-AC3-CAV1 by CAP1 depletion or resistin treatment

CAP1 knockdown led to increased expression of ICAM-1 and VCAM-1, enhancing trans-endothelial migration of the circulating monocytes. Such effects of CAP1 depletion was well reproduced by resistin treatment that also destroys the triple complex. ICAM-1 and VCAM-1 have pivotal roles during adhesion of circulating leukocytes on endothelial surface[31]. Therefore, it is expected that CAP1 depletion augments trans-endothelial migration through ICAM-1 and VCAM-1 over-expression. ICAM-1 is also involved in the transcytosis of leukocytes independently of its role in adhesion. When leukocytes are adhere to ECs, apical ICAM-1 is translocated to F-actin-rich caveolae and supports the transcytosis of leukocytes into ECs through internalization of caveolin[32]. Thus, increased ICAM-1 expression may partly enhance trans-endothelial migration through transcytosis. Given that CAP1 is involved in F-actin

regulation, its uncoupling from CAV1 might further enhance monocyte extravasation by modulating cytoskeletal dynamics.

To confirm the pathophysiological relevance of CAP1 in ECs *in vivo*, first we used CAP1$^{+/-}$ mice. We observed the enhanced monocyte extravasation and higher macrophage infiltration in the local inflamed tissues in CAP1$^{+/-}$ mice. Interestingly, however, edema severity was milder despite of the increased macrophage infiltration, suggesting impaired monocyte function in CAP1$^{+/-}$ mice, which we confirmed in this study. Thus to exclude the confounding effects of the dysfunctional monocytes, we repeated the *in vivo* experiment using CAP1$^{+/-}$ mice that received the normal monocytes by bone marrow transplantation from WT mice. Introducing normal monocytes into CAP1$^{+/-}$ mice resulted in exacerbated macrophage infiltration as well as edema formation, confirming that endothelial CAP1 depletion directly enhances monocyte extravasation and inflammation.

Perspectives

Our findings highlight CAP1 as a gatekeeper against inflammation in ECs by forming a triple complex with AC3/AC6 and CAV1 within lipid rafts and suppressing AC activity, which maintains the normal ECs' barrier function against monocyte infiltration. When resistin binds CAP1, this CAP1-AC3-CAV1 complex disassembles, leading to AC activation, adhesion molecule upregulation, and increased inflammation. In contrast, in monocytes, AC4 and AC7 are localized in non-lipid-rafts and remain unsuppressed by CAP1/CAV1, allowing resistin to directly activate AC and induce cytokine release. This dual mechanism of the resistin-CAP1 axis highlights distinct inflammatory pathways in ECs and monocytes. Targeting this axis may offer new strategies to mitigate chronic inflammation in metabolic syndrome where resistin is increased and resistin-CAP1 axis is activated.

Declarations

Acknowledgements

This work was supported by the grant of the Korea Health Technology R&D Project funded by the Ministry of Health & Welfare, Republic of Korea (HI16C0225), "Korea Research-Driven Hospital" **(HI14C1277)** through the Korea Health Industry Development Institute and the Korea Health Technology Research and Development Project "Strategic Center of Cell and Bio Therapy" **(HI 17C2085) and supported by the National Research Foundation of Korea (NRF) grant funded by the Korea government(MSIT) (RS-2024-00359519).**

Authorship Contributions

S.L., H.M.Y., Y.W.K., and H.S.K. designed research studies. H.C.L., S.L., Y.J.K., D.S., J.K., J.L., H.D.J., and E.B.C. conducted experiments and acquired data. S.L., H.C.L., Y.J.K., and Y.W.K. analyzed data and S.L., Y.J.K., Y.W.K., and H.S.K. wrote the manuscript.

Disclosure of Conflicts of interest

The authors have no conflicts of interest or financial disclosures to declare.

References

1. Gregor, M. F. & Hotamisligil, G. S. Inflammatory mechanisms in obesity. *Annu Rev Immunol* **29**, 415-445 (2011).
2. Chae, C. W. & Kwon, Y. W. Cell signaling and biological pathway in cardiovascular diseases. *Arch Pharm Res* **42**, 195-205 (2019).
3. Bokarewa, M., Nagaev, I., Dahlberg, L., Smith, U. & Tarkowski, A. Resistin, an adipokine with potent proinflammatory properties. *J Immunol* **174**, 5789-5795 (2005).
4. Reilly, M. P. *et al.* Resistin is an inflammatory marker of atherosclerosis in humans. *Circulation* **111**, 932-939 (2005).
5. Hivert, M. F. *et al.* Association of variants in RETN with plasma resistin levels and diabetes-related traits in the Framingham Offspring Study. *Diabetes* **58**, 750-756 (2009).
6. Chen, B. H. *et al.* Circulating levels of resistin and risk of type 2 diabetes in men and women: results from two prospective cohorts. *Diabetes Care* **32**, 329-334 (2009).
7. Steppan, C. M. *et al.* The hormone resistin links obesity to diabetes. *Nature* **409**, 307-312 (2001).
8. Cho, Y. *et al.* Adipokine resistin is a key player to modulate monocytes, endothelial cells, and smooth muscle cells, leading to progression of atherosclerosis in rabbit carotid artery. *J Am Coll Cardiol* **57**, 99-109 (2011).
9. Lee, S. *et al.* Adenylyl cyclase-associated protein 1 is a receptor for human resistin and mediates inflammatory actions of human monocytes. *Cell Metab* **19**, 484-497 (2014).
10. Yang, H. M. *et al.* Resistin impairs mitochondrial homeostasis via cyclase-associated protein 1-mediated fission, leading to obesity-induced metabolic diseases. *Metabolism* **138**, 155343 (2023).
11. Yang, H.-M. *et al.* Resistin Regulates Inflammation and Insulin Resistance in Humans via the Endocannabinoid System. *Research* **7**, 0326 (2024).
12. Hubberstey, A. V. & Mottillo, E. P. Cyclase-associated proteins: CAPacity for linking signal transduction and actin polymerization. *Faseb j* **16**, 487-499 (2002).
13. Jang, H. D. *et al.* Cyclase-associated protein 1 is a binding partner of proprotein convertase subtilisin/kexin type-9 and is required for the degradation of low-density lipoprotein receptors by proprotein convertase subtilisin/kexin type-9. *Eur Heart J* **41**, 239-252 (2020).
14. Shin, D. *et al.* PCSK9 stimulates Syk, PKCδ, and NF-κB, leading to atherosclerosis progression independently of LDL receptor. *Nat Commun* **15**, 2789 (2024).
15. Yang, H. M. *et al.* Resistin Regulates Inflammation and Insulin Resistance in Humans via the Endocannabinoid System. *Research (Wash D C)* **7**, 0326 (2024).

16. Verma, S. *et al.* Resistin promotes endothelial cell activation: further evidence of adipokine-endothelial interaction. *Circulation* **108**, 736-740 (2003).
17. Hsu, W. Y. *et al.* Resistin induces monocyte-endothelial cell adhesion by increasing ICAM-1 and VCAM-1 expression in endothelial cells via p38MAPK-dependent pathway. *J Cell Physiol* **226**, 2181-2188 (2011).
18. Willoughby, D. & Cooper, D. M. Organization and Ca2+ regulation of adenylyl cyclases in cAMP microdomains. *Physiol Rev* **87**, 965-1010 (2007).
19. Wang, C., Zhou, G. L., Vedantam, S., Li, P. & Field, J. Mitochondrial shuttling of CAP1 promotes actin- and cofilin-dependent apoptosis. *J Cell Sci* **121**, 2913-2920 (2008).
20. Peche, V. *et al.* CAP2, cyclase-associated protein 2, is a dual compartment protein. *Cell Mol Life Sci* **64**, 2702-2715 (2007).
21. Toya, Y., Schwencke, C., Couet, J., Lisanti, M. P. & Ishikawa, Y. Inhibition of adenylyl cyclase by caveolin peptides. *Endocrinology* **139**, 2025-2031 (1998).
22. Allen, J. A. *et al.* Caveolin-1 and lipid microdomains regulate Gs trafficking and attenuate Gs/adenylyl cyclase signaling. *Mol Pharmacol* **76**, 1082-1093 (2009).
23. Head, B. P. *et al.* Microtubules and actin microfilaments regulate lipid raft/caveolae localization of adenylyl cyclase signaling components. *J Biol Chem* **281**, 26391-26399 (2006).
24. Ostrom, R. S. *et al.* Receptor number and caveolar co-localization determine receptor coupling efficiency to adenylyl cyclase. *J Biol Chem* **276**, 42063-42069 (2001).
25. Baumer, Y., Spindler, V., Werthmann, R. C., Bünemann, M. & Waschke, J. Role of Rac 1 and cAMP in endothelial barrier stabilization and thrombin-induced barrier breakdown. *J Cell Physiol* **220**, 716-726 (2009).
26. Raker, V. K., Becker, C. & Steinbrink, K. The cAMP Pathway as Therapeutic Target in Autoimmune and Inflammatory Diseases. *Front Immunol* **7**, 123 (2016).
27. Bock, A. *et al.* Optical Mapping of cAMP Signaling at the Nanometer Scale. *Cell* **182**, 1519-1530.e1517 (2020).
28. Perrot, C. Y., Sawada, J. & Komatsu, M. Prolonged activation of cAMP signaling leads to endothelial barrier disruption via transcriptional repression of RRAS. *Faseb j* **32**, fj201700818RRR (2018).
29. Hadad, N., Tuval, L., Elgazar-Carmom, V., Levy, R. & Levy, R. Endothelial ICAM-1 protein induction is regulated by cytosolic phospholipase A2α via both NF-κB and CREB transcription factors. *J Immunol* **186**, 1816-1827 (2011).
30. Gao, N., Hibi, Y., Cueno, M., Asamitsu, K. & Okamoto, T. A-kinase-interacting protein 1 (AKIP1) acts as a molecular determinant of PKA in NF-kappaB signaling. *J Biol Chem* **285**, 28097-28104 (2010).
31. Ley, K., Laudanna, C., Cybulsky, M. I. & Nourshargh, S. Getting to the site of inflammation: the leukocyte adhesion cascade updated. *Nat Rev Immunol* **7**, 678-689 (2007).
32. Millán, J. *et al.* Lymphocyte transcellular migration occurs through recruitment of endothelial ICAM-1 to caveola- and F-actin-rich domains. *Nat Cell Biol***8**, 113-123 (2006).

Figures

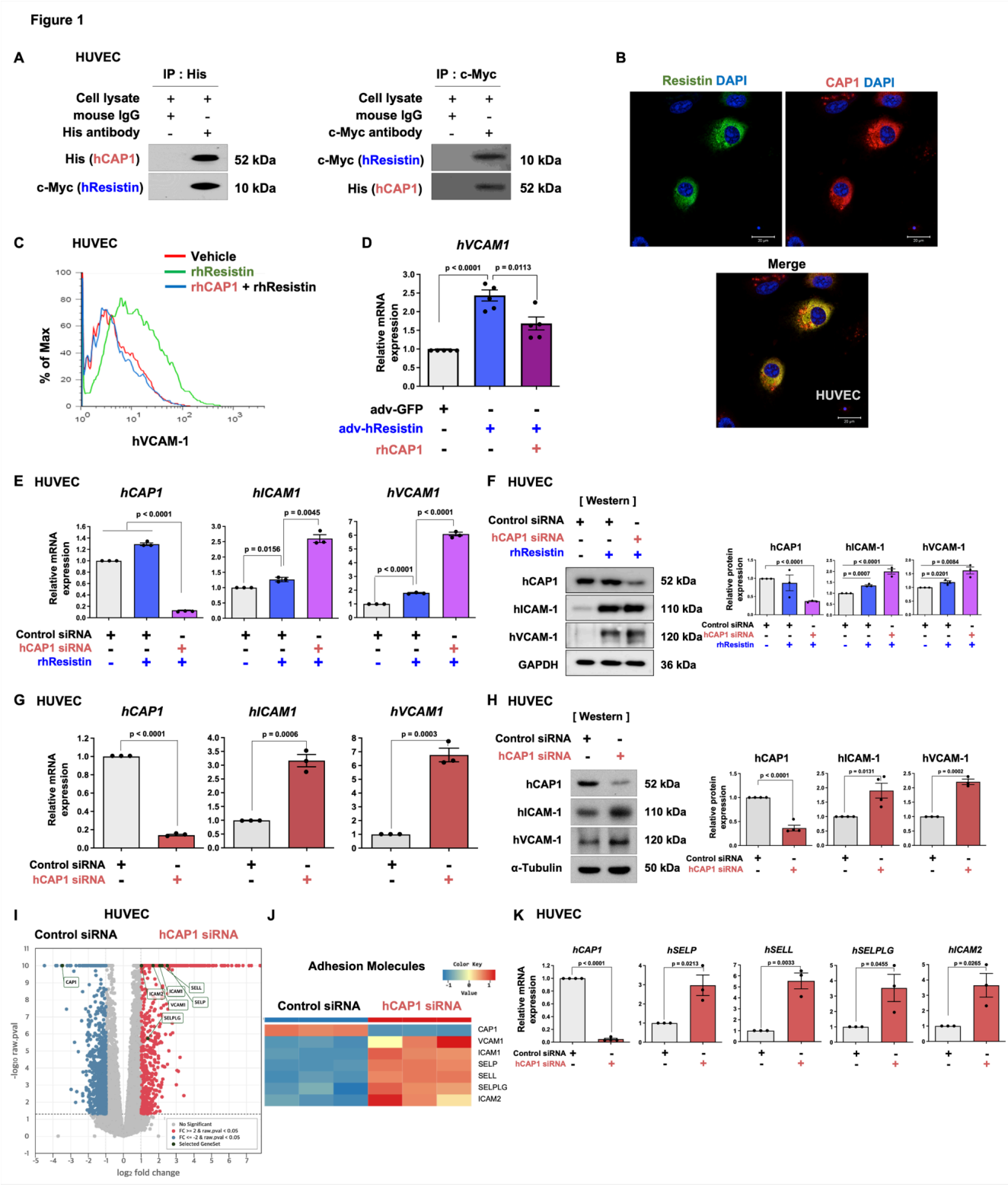


Figure 1

CAP1, a functional receptor of human resistin, is essential for regulating adhesion molecule expression in human ECs

(A) Co-immunoprecipitation (Co-IP) analysis showing the direct interaction between resistin and CAP1 in HUVECs. Cells were co-transfected with His-tagged CAP1 and c-Myc-tagged resistin. Lysates were immunoprecipitated (IP) with anti-His or anti-c-Myc antibodies and immunoblotted (IB) as indicated.

(B) Representative confocal microscopy images showing the intracellular co-localization of transfected mouse Fc-tagged resistin (green) and CAP1 (red) in HUVECs. Nuclei were stained with DAPI (blue). Scale bar: 20 μm.

(C, D) Neutralization of resistin-induced inflammation by soluble CAP1.I) Flow cytometric analysis of surface VCAM-1 expression and (D) qRT-PCR analysis of VCAM1 mRNA levels. HUVECs were treated with recombinant human resistin (rhResistin, 50 ng/mL) in the presence or absence of recombinant human CAP1 protein (rhCAP1, 250 ng/mL).

(E, F) Effect of CAP1 knockdown on resistin signaling (E) qRT-PCR and (F) Western blot analysis showing that CAP1 silencing significantly enhances resistin-induced expression of ICAM-1 and VCAM-1 compared to control siRNA.

(G) qRT-PCR and (H) Western blot analysis demonstrating that genetic depletion of CAP1 alone is sufficient to markedly upregulate ICAM-1 and VCAM-1 expression.

(I) Volcano plot and (J) Heatmap derived from RNA sequencing analysis comparing HUVECs transfected with control siRNA versus CAP1 siRNA. The data reveal a broad upregulation of genes encoding cell adhesion molecules (e.g., ICAM1, VCAM1, SELP, SELL) in CAP1-depleted cells. (K) qRT-PCR validation of selected adhesion molecules (SELP, SELL, SELPLG, ICAM2) identified from the RNA-seq analysis. Data are presented as mean ± SD from three independent experiments (n=3). ns: not significant, $P < 0.05$, *$P < 0.01$, **$P < 0.001$.

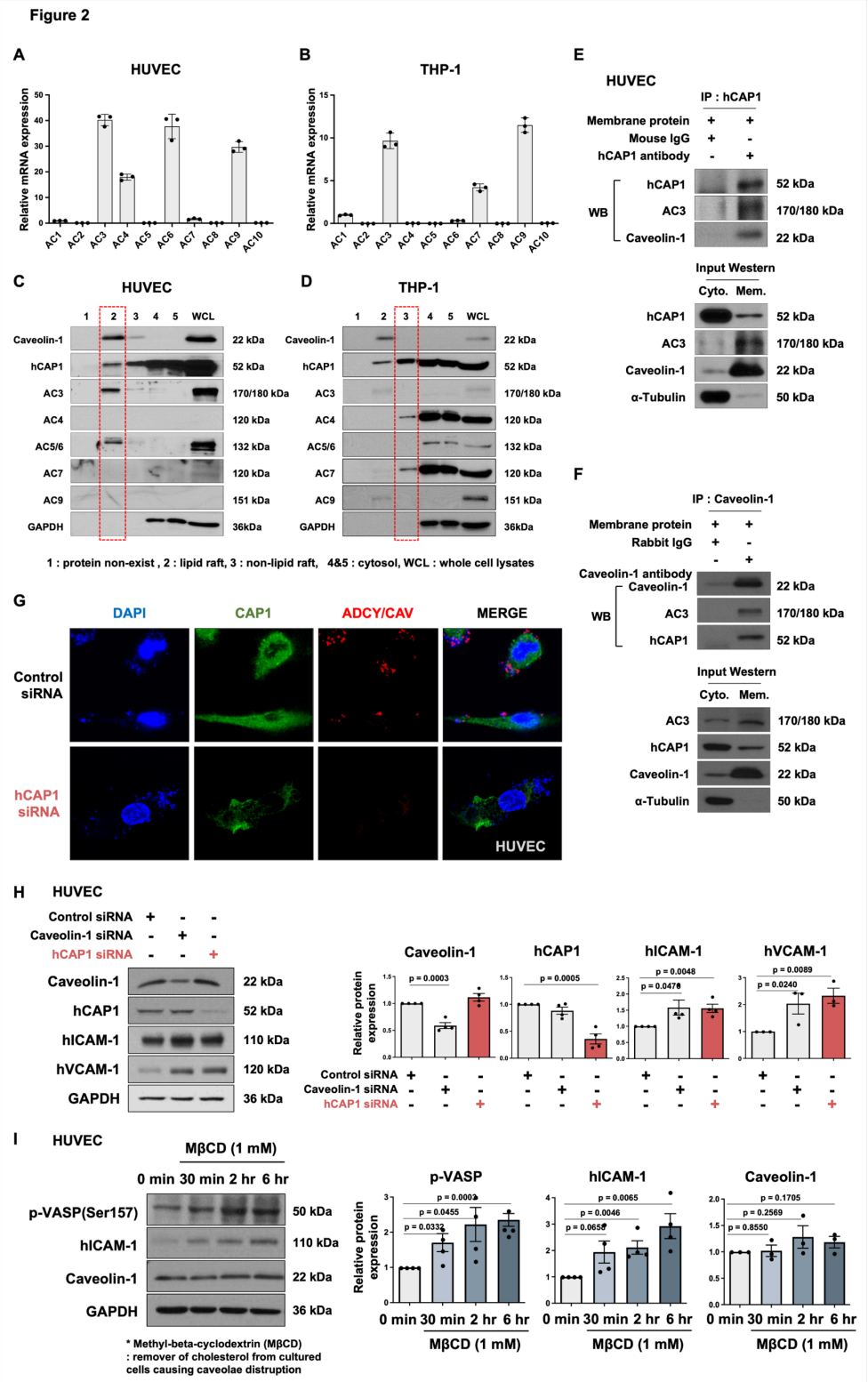


Figure 2

CAP1 binds to adenylyl cyclase-3 or -6 in the caveolin1-enriched lipid raft membrane in ECs

(A, B) mRNA expression of adenylyl cyclase isoforms in HUVECs and THP-1 cells. AC3, AC4, AC6, and AC9 are predominant in HUVECs, AC3, AC7, and AC9 in THP-1. Data normalized to GAPDH (n = 3).

(C, D) Protein expression and subcellular localization of AC isoforms. In HUVECs, AC3/6 co-localized with CAV1 in lipid raft fractions (2nd lane), while in THP-1, AC7 was found in non-lipid raft (3rd lane). CAP1 was broadly distributed (n = 3).

(E, F) Co-immunoprecipitation demonstrates a CAP1-AC3-CAV1 complex at the plasma membrane of HUVECs (n = 3).

(G) Scaffolding role of CAP1. Proximity Ligation Assay (PLA) visualizing the in situ interaction between AC3 and Caveolin-1 (red dots). CAP1 knockdown (indicated by reduced green signal) markedly diminishes the PLA signal, demonstrating that CAP1 is required to scaffold the AC3-Caveolin-1 interaction.

(H) Induction of adhesion molecules by complex loss. Western blot analysis showing that genetic depletion of either Caveolin-1 or CAP1 is sufficient to upregulate ICAM-1 and VCAM-1 protein expression, mimicking the inflammatory effects of resistin.

(I) Effect of lipid raft disruption. HUVECs treated with methyl-β-cyclodextrin (MβCD, 1 mM) exhibit a time-dependent increase in p-VASP (Ser157) and ICAM-1 expression. This gradual accumulation kinetics suggests that structural disruption of caveolae leads to the progressive de-suppression of AC signaling. Data are presented as mean ± SEM from three independent experiments (n=3). $P < 0.05$, *$P < 0.01$ vs. vehicle or control siRNA group.

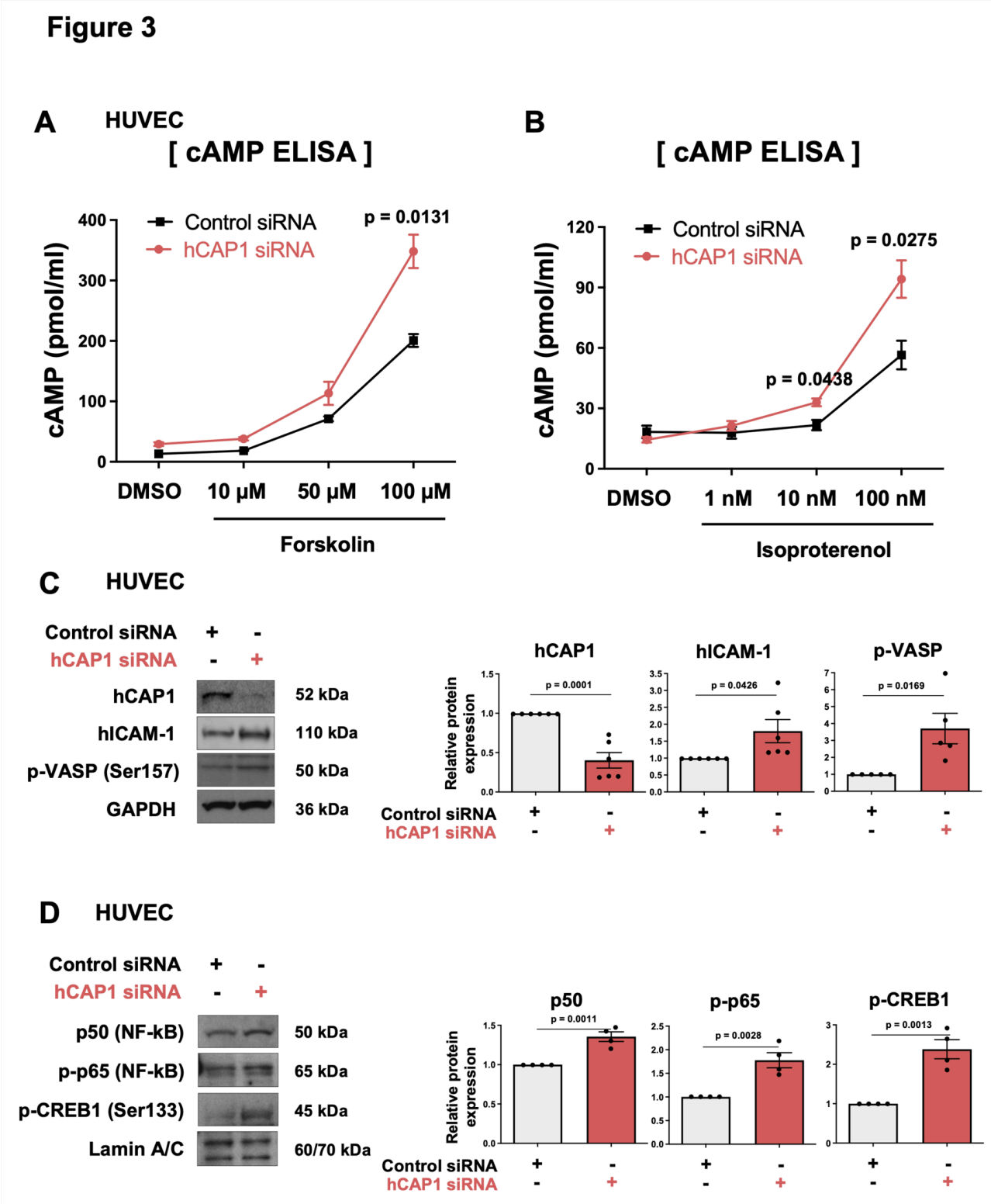


Figure 3

CAP1 depletion promotes adhesion molecule expression via the cAMP-PKA-CREB and NF-κB signaling pathways in ECs.

(A–B) Disinhibition of cAMP synthesis. (A, B) cAMP levels in control or CAP1-silenced HUVECs treated with (A) Forskolin or (B) Isoproterenol. Note that CAP1 knockdown elevates basal cAMP and

hypersensitizes cells to AC stimulation.

(C, D) Activation of downstream signaling pathways. (C) Western blot analysis of whole-cell lysates showing increased expression of ICAM-1 and phosphorylation of VASP (Ser157) upon CAP1 knockdown. (D) Nuclear fractionation analysis showing nuclear accumulation of NF-κB subunits (p50, p-p65) and phosphorylation of CREB (Ser133). Lamin A/C served as a nuclear loading control. Data are presented as mean ± SEM (n=3). P < 0.05, *P < 0.01 vs. vehicle or control siRNA group.

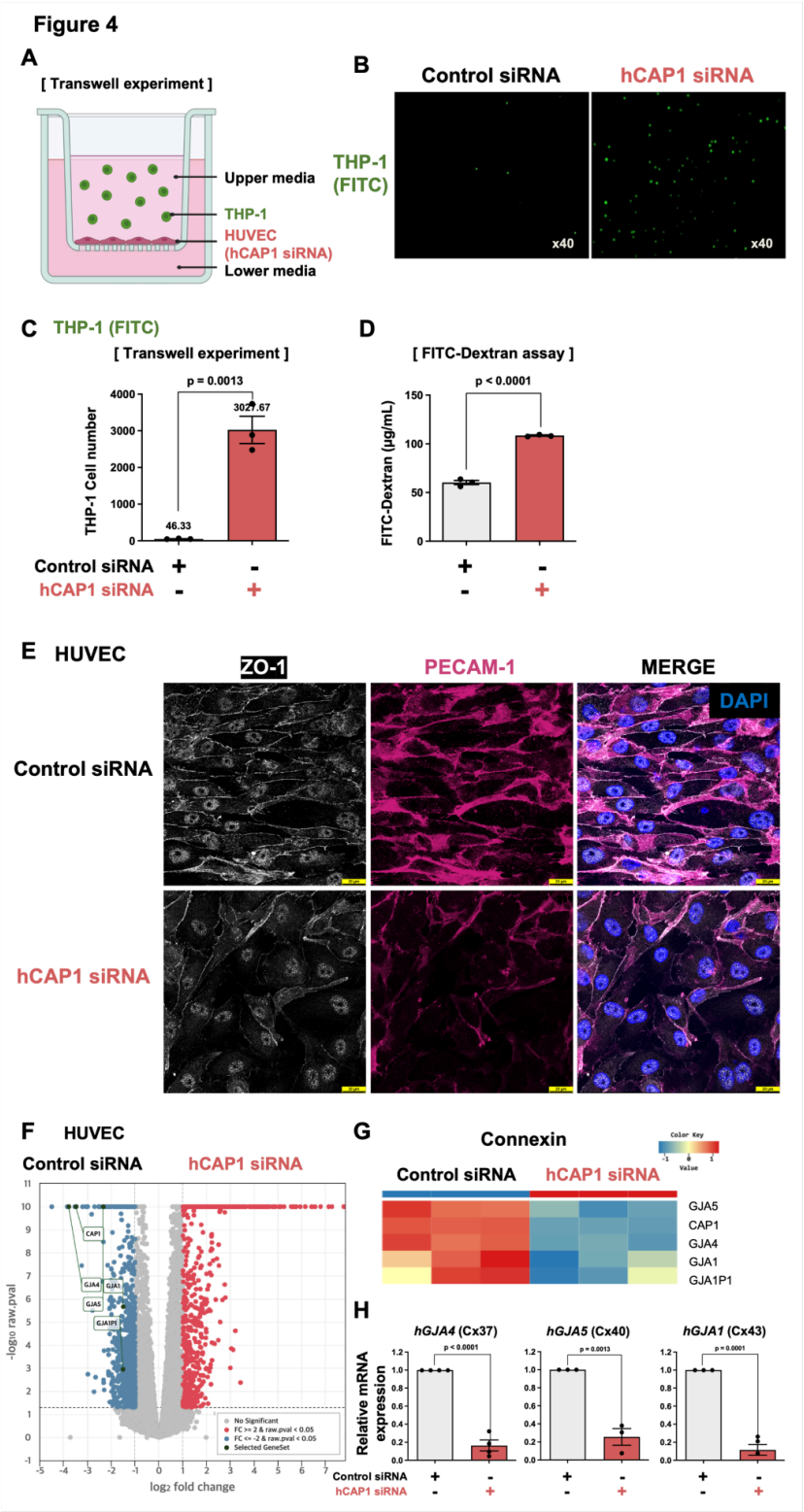


Figure 4

CAP1 depletion impairs endothelial barrier integrity and promotes monocyte trans-endothelial migration.

(A–C) Increased leukocyte transmigration. (A) Schematic representation of the trans-endothelial migration assay. HUVECs were transfected with CAP1 siRNA. Schematic diagram created with BioRender. (B) representative fluorescence images of transmigrated monocytes, and (C) Quantification.

(D, E) Endothelial barrier disruption and junctional fragmentation. (D) Paracellular permeability assessed by FITC-dextran flux. (E) Representative immunofluorescence images showing tight junctions (ZO-1, white) and adherens junctions (PECAM-1, magenta). Note the discontinuous junctional staining in CAP1-silenced cells.

(F–H) Transcriptomic reprogramming via RNA sequencing. (F) Volcano plot comparing gene expression profiles between control and CAP1 siRNA-transfected HUVECs. (G, H) Downregulation of gap junction proteins. (G) Heatmap and (H) qRT-PCR results demonstrating the significant reduction of gap junction protein genes (hGJA4/Cx37, hGJA5/Cx40, hGJA1/Cx43) in CAP1-deficient cells, indicating impaired intercellular communication.

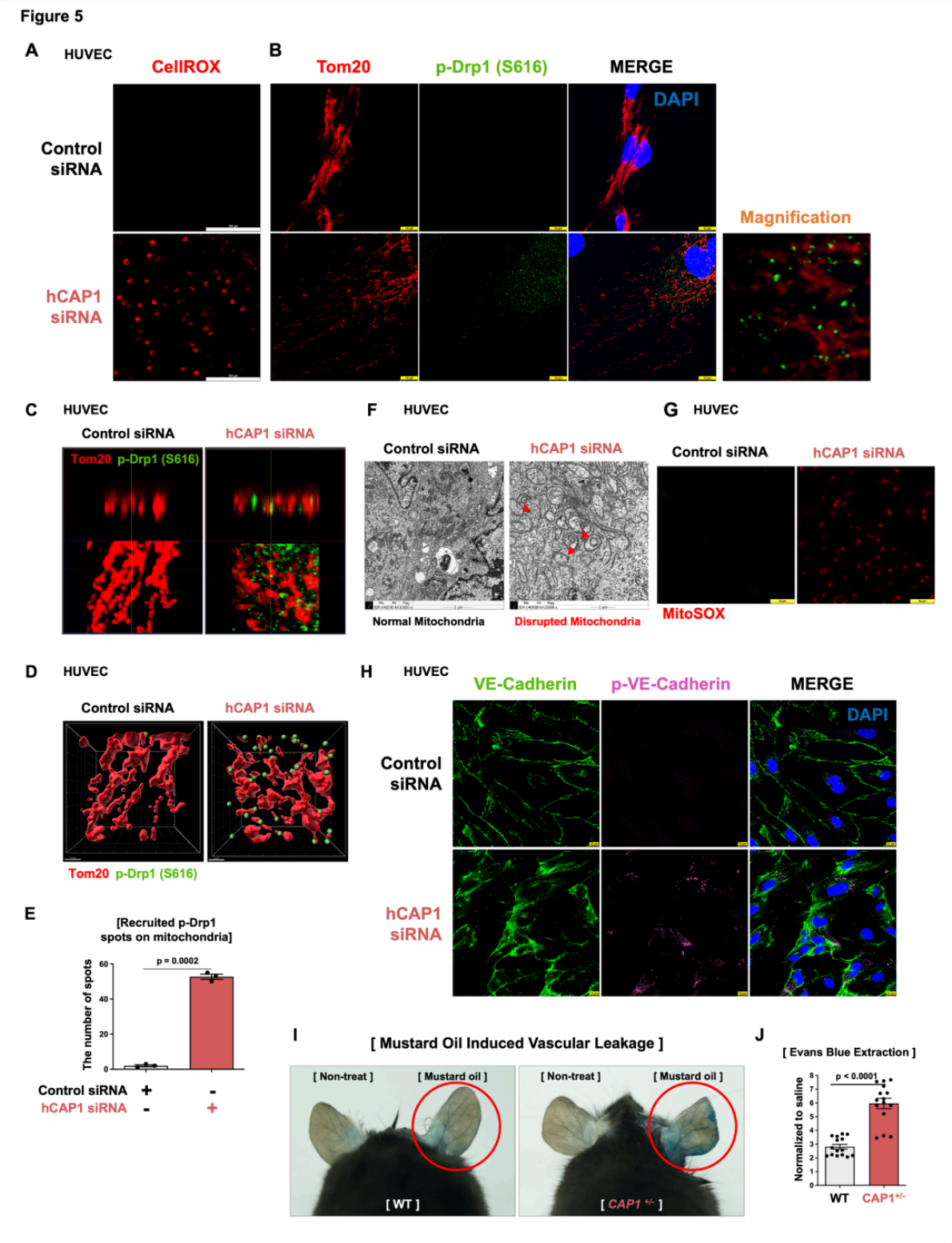


Figure 5

Disruption of complex CAP1–AC3-CAV1 by CAP1 knockdown induces mitochondrial fission and oxidative stress, leading to ECs' barrier breakdown

(A-G) Mitochondrial oxidative stress and structural collapse. (A) Detection of cellular ROS using CellROX (red). (B, C) Confocal microscopy analysis (B) and 3D reconstruction (C) showing the recruitment of

phosphorylated Drp1 (S616, green) to mitochondria (Tom20, red), indicating active fission. (D) IMARIS 3D surface rendering visualizing the spatial distribution and recruitment of p-Drp1 (S616, green spheres) on mitochondria (Tom20, red surface). (E) Quantification of the number of recruited p-Drp1 spots on mitochondria (F) Ultrastructural analysis by transmission electron microscopy (TEM) revealing mitochondrial swelling and cristolysis (red arrowheads) in CAP1-silenced cells. (G) Evaluation of mitochondrial-specific superoxide (ROS) production using MitoSOX Red indicator.

(H) Junctional destabilization via VE-Cadherin phosphorylation. Immunofluorescence staining for total VE-Cadherin (green) and phosphorylated VE-Cadherin (magenta), a marker of junction disassembly.

(I, J) Aggravated vascular permeability *in vivo*. (F) Representative images of mustard oil-induced vascular leakage in the ears of WT and CAP1$^{+/-}$ mice. (G) Quantification of vascular permeability determined by Evans Blue dye extraction. Data are presented as mean ± SEM (n=3). $P < 0.05$, *$P < 0.01$ vs. control siRNA or vehicle-treated group.

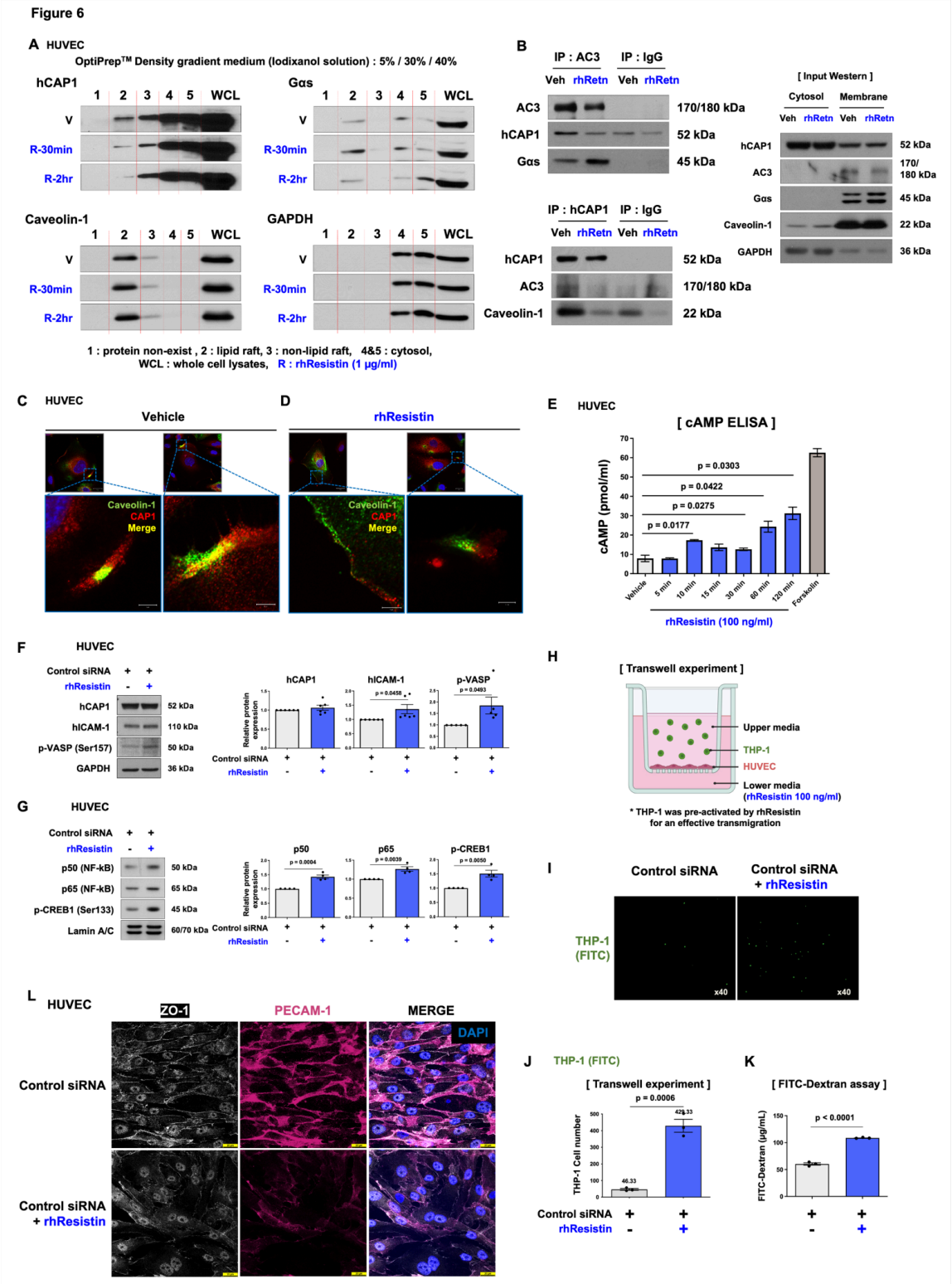


Figure 6

Resistin disassembles CAP1-AC3-CAV1 complex, leading to activation of adenylyl cyclase in ECs

(A) Dynamic subcellular redistribution. Western blot analysis of Opti-prep density gradient fractions showing the translocation of CAP1 from lipid rafts (lane 2) to non-lipid raft/cytosolic fractions (lanes 3–5) and the concurrent recruitment of Gαs to the lipid raft fraction upon resistin treatment (1 μg/mL).

(B) Disassembly of the inhibitory complex and Gαs coupling. Co-immunoprecipitation (Co-IP) assays revealing that resistin treatment dissociates CAP1 and Caveolin-1 from AC3 while significantly promoting the physical interaction between AC3 and Gαs. Note that immunoprecipitation with anti-CAP1 antibody confirms the simultaneous loss of Caveolin-1 and AC3 binding upon resistin exposure.

(C, D) Visualization of complex dissociation. Representative immunofluorescent images showing the co-localization of CAP1 (red) and Caveolin-1 (green) at the plasma membrane in vehicle-treated cells (C), which is markedly disrupted after 30 minutes of resistin exposure (D). Scale bars: 20 μm (large), 5 μm (inset).

(E) Time-course analysis of intracellular cAMP levels in HUVECs treated with resistin (100 ng/mL). Data are presented as mean ± SD (n=3).

(F) Western blot and quantification of hCAP1, hICAM-1, and p-VASP (Ser157) in rhResistin-treated HUVECs. (G) Western blot and quantification of nuclear p50, p65, and p-CREB1 (Ser133) in rhResistin-treated HUVECs.

(H–J) Increased leukocyte transmigration. (H) Schematic diagram created with BioRender. (I) Representative fluorescence images of transmigrated monocytes, and (J) Quantification.

(K) Paracellular permeability assessed by FITC-dextran flux. (L) Representative immunofluorescence images showing tight junctions (ZO-1, white) and adherens junctions (PECAM-1, magenta). HUVECs were treated with rhResistin.

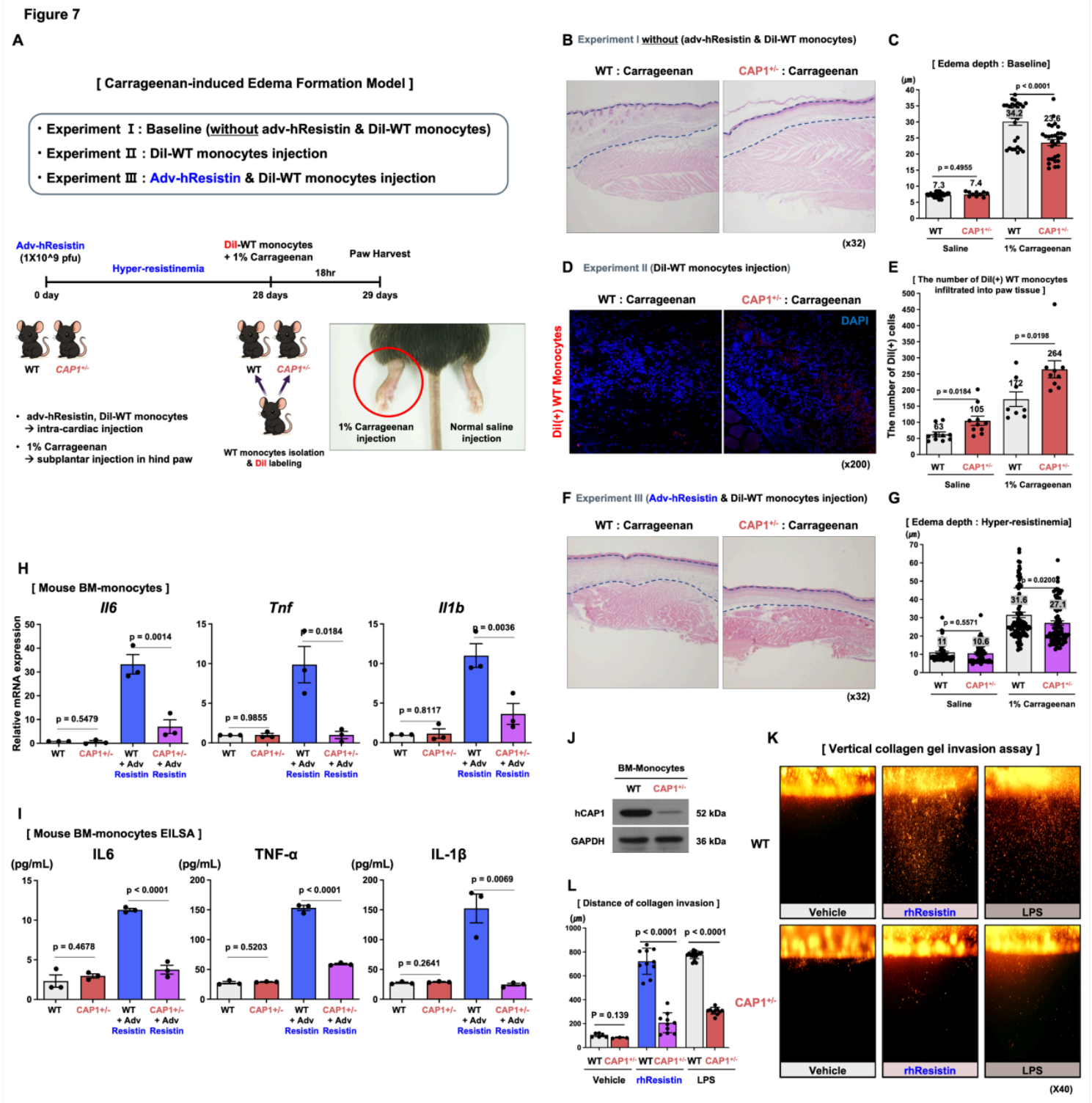


Figure 7

Phenotype of CAP hetero-knockout mice in the edema formation model. The enhanced monocyte extravasation due to CAP1-knockdown in ECs, but less inflammation due to dysfunctional monocytes with CAP1-knockdown.

(A) Schematic overview of three sequential experimental designs using the carrageenan-induced paw edema model.

Experiment I (Baseline): λ-carrageenan (1%, 50 µL) was injected subplantarly into WT or CAP1$^{+/-}$ mice without exogenous monocyte transfer.

Experiment II (Monocyte tracing): For tracing purpose, DiI-labeled WT monocytes were injected via intra-cardiac route into WT or CAP1$^{+/-}$ mice, followed by subplantar λ-carrageenan injection.

Experiment III (Hyper-resistinemia conditions): Hyper-resistinemia was induced by adenoviral overexpression of human resistin

(B, C) Enhanced monocyte infiltration in CAP1$^{+/-}$ mice. (B) Representative immunofluorescence images of DiI-labeled WT monocytes (red) infiltrating the inflamed paw tissue. Nuclei were stained with DAPI (blue). (C) Quantification of the number of infiltrated DiI(+) monocytes (n = 4). (D–G) Paradoxical attenuation of edema in CAP1$^{+/-}$ mice.

(D, E) Representative H&E-stained sections (D) and quantification of edema depth (E) under baseline conditions (Experiment I).

(F, G) Representative H&E-stained sections (F) and quantification of edema depth (G) under hyper-resistinemic conditions (Experiment III). Note that despite increased monocyte infiltration, edema formation is reduced in CAP$^{1+/-}$ mice due to monocyte dysfunction. (n = 4–8).

(H, I) Impaired inflammatory response in CAP1$^{+/-}$ monocytes. (H) qRT-PCR analysis of inflammatory cytokines (Il6, Tnf, Il1b) and (I) ELISA measurement of secreted cytokines (IL-6, TNF-α, IL-1β) in bone marrow-derived monocytes stimulated with rhResistin (100 ng/mL).

(J) Confirmation of CAP1 reduction. Western blot analysis showing reduced CAP1 protein levels in bone marrow monocytes isolated from CAP1$^{+/-}$ mice compared to WT.

(K, L) Defective chemotactic migration. (K) Representative images of the vertical collagen gel invasion assay. (L) Quantification of the invasion distance toward rhResistin or LPS (100 ng/mL). CAP1$^{+/-}$ monocytes exhibit significantly impaired motility. Data are presented as mean ± SD (n=3). ns: not significant, *p < 0.05, **p < 0.01, ***p < 0.001.

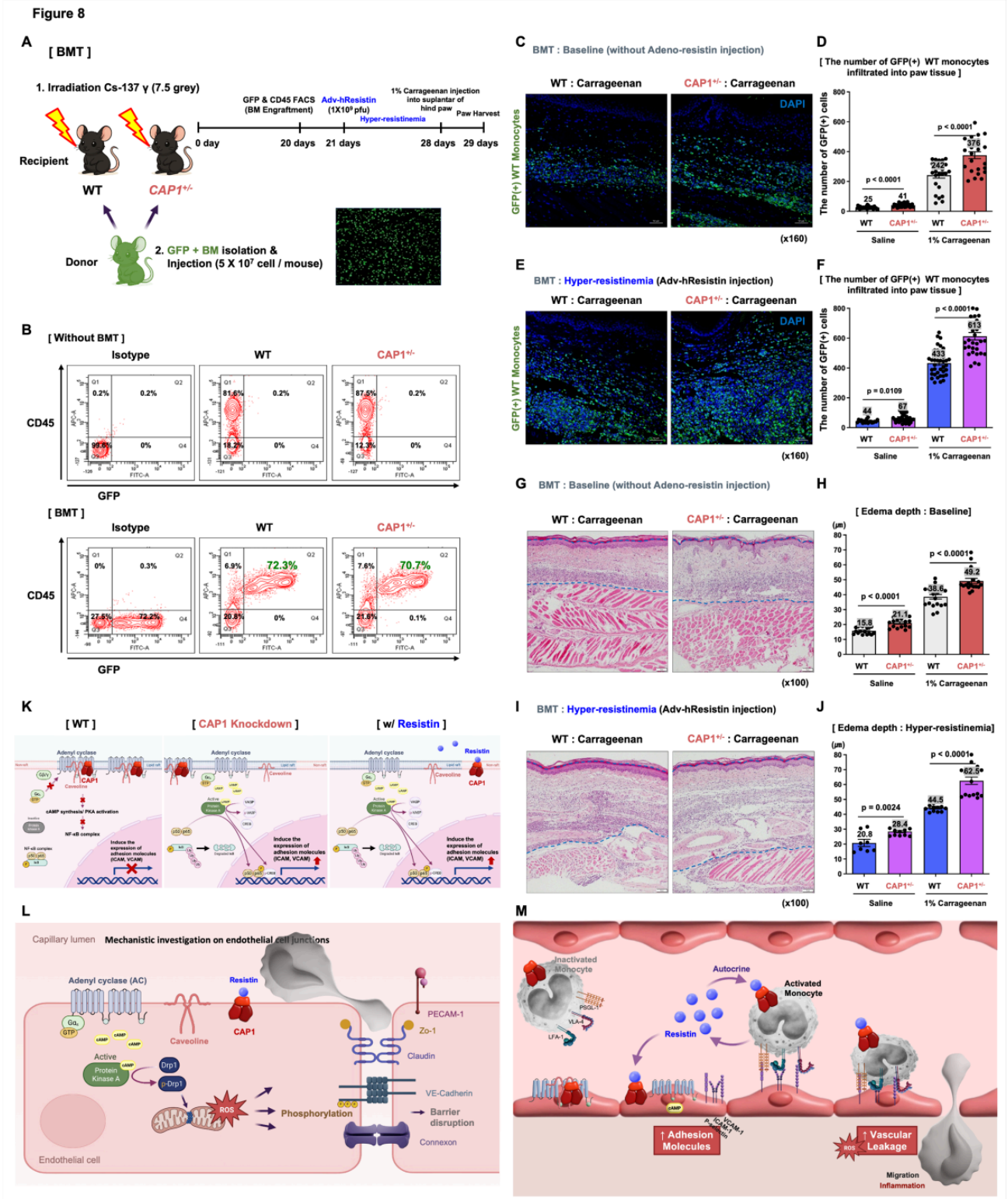


Figure 8

Phenotype of CAP1 hetero-knockout mice receiving normal monocytes from WT bone marrow transplantation in the edema formation model. Selective endothelial CAP1 deficiency promotes monocyte infiltration and local inflammation.

(A) Generation of bone marrow chimeric mice. Schematic timeline of the bone marrow transplantation (BMT) procedure. Lethally irradiated WT or CAP1$^{+/-}$ recipient mice were reconstituted with bone marrow cells from GFP-transgenic WT donors (5×10^{7} cells/mouse). After 4 weeks of recovery, mice were subjected to hyper-resistinemia (Ad-hResistin) and carrageenan-induced inflammation.

(B) Validation of engraftment efficiency. Flow cytometric analysis of peripheral blood cells stained for CD45 and GFP. Successful reconstitution was confirmed by the high percentage (>70%) of GFP(+) donor-derived leukocytes in BMT recipients compared to non-transplanted controls.

(C–F) Aggravated tissue edema in endothelial CAP1-deficient mice. Representative immunofluorescence images and quantification of infiltrating GFP(+) WT monocytes (green) in the inflamed paws of WT and CAP1$^{+/-}$ recipients under (C, D) baseline or (E, F) hyper-resistinemic conditions. Nuclei were stained with DAPI (blue). Endothelial CAP1 deficiency alone was sufficient to promote massive leukocyte extravasation.

(G-J) Representative H&E-stained paw sections and quantification of edema depth in WT and CAP1$^{+/-}$ recipients under (G, H) baseline or (I, J) hyper-resistinemic conditions. Unlike global CAP1$^{+/-}$ mice (Figure 7), CAP1$^{+/-}$ recipients with normal WT monocytes exhibited significantly severe edema. Increased infiltration of WT monocytes. Data are presented as mean ± SEM (n=6 per group). $P < 0.05$, *$P < 0.01$, **$P < 0.001$.

(K–M) Proposed molecular mechanism. (K) Schematic of the CAP1-regulated cAMP-PKA signaling axis. (K) Detailed mechanism illustrating how PKA-mediated Drp1 activation and subsequent ROS generation lead to VE-Cadherin phosphorylation and barrier opening. (M) Integrated model of the resistin-CAP1 axis facilitating monocyte extravasation during vascular inflammation. Schematic diagram created with BioRender.

Supplementary Files

This is a list of supplementary files associated with this preprint. Click to download.

- CAP1ECanimationabstract.pptx
- SupplementalMaterialandMethod20260406.docx
- SupplementalMaterialandMethod20260408.docx